119 ON THE STRUCTURE AND DYNAMICS OF INDIAN MONSOON DEPRESSIONS

Kieran M. R. Hunt* Andrew G. Turner

February 1, 2016

1 INTRODUCTION

The Indian monsoon trough region experiences 3-6 synoptic scale cyclonic depressions (IMDs) passing through it during the average summer. The majority of these depressions originate over the head of the Bay of Bengal, usually propagating northwestward onto the Indian subcontinent, lasting an average of 4-5 days with the criterion that they have surface winds between 8.5 m s^{-1} and 16.5 m s^{-1}(e.g. Godbole, 1977; Saha et al., 1981; Sarker and Choudhary, 1988; Stano et al., 2002).

Detailed investigation of depression structure in and around the Indian monsoon trough region has been performed previously (e.g. Godbole, 1977; Ding, 1981; Ding et al., 1984; Sarker and Choudhary, 1988; Prasad et al., 1990; Stano et al., 2002). Although the largest composite generated was of forty depressions (split into four categories of intensity) by Prasad et al. (1990), they only considered wind, and included analysis of satellite-imaged cloud cover on a case-study basis. Sarker and Choudhary (1988) analysed a number of variables (temperature, moisture, winds, vorticity) of a 27-depression composite based on events during 1961-74, but their data were interpolated from a relatively sparse array of radiosonde stations, all over land. More recently, Stano et al. (2002) conducted hydrometeor analysis on three depressions from 1999.

With the advent of extensive satellite and reanalysis datasets, a truly thorough analysis of a large depression composite over land and sea has now become a possibility. Hurley and Boos (2015) considered a 117-depression composite for 1979-2013, but they did not go into specific detail, instead considering the worldwide climatology of monsoon depressions and examining the winds, potential temperature, and potential vorticity of Indian monsoon depressions. Boos et al. (2015) looked at a potential vorticity analysis of the same dataset. Their analysis also contains more depressions because they consider those originating over the Arabian Sea and inland, whereas we do not.

2 TRACKING

To automate the collection of data on depressions, feature tracking software was written, as summarised in Fig. 1. Due to the complex orography north of the trough, and the sea-to-land transitions of depressions, we could not rely solely on any particular criterion, so a filtering procedure was carried out on relative vorticity, geopotential height and wind speed.

For each six-hourly timestep, the tracking software finds a relative vorticity maximum at 800 hPa, above a threshold of $1{\times}10^{-5}$ s^{-1}. It then eliminates all cases without a nearby synoptic scale surface low (negative surface pressure anomaly relative to a 21-day climatology), or failing the wind threshold criterion for depressions. Use of the 800 hPa level reduces boundary layer effects from the Himalayas while sampling the vortical core. Consecutive reanalysis outputs containing depression candidates are then connected, as long as the candidate has not moved too far between frames, and locations, times and headings are recorded.

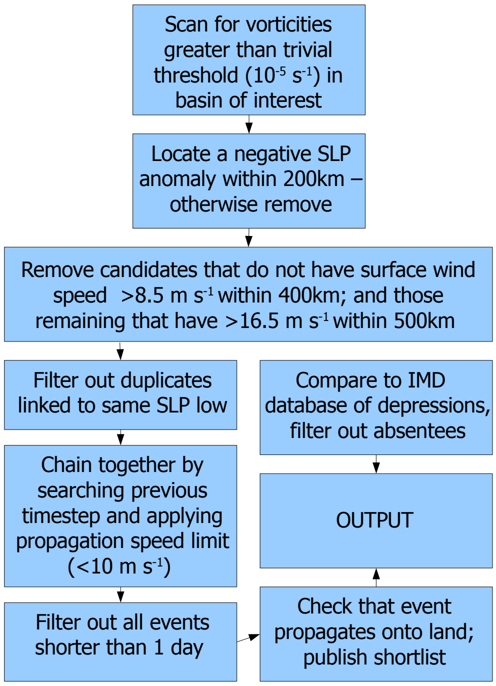

Figure 1: Flowchart outlining the key stages of the tracking algorithm.

Filtering is applied to ensure consecutive relative vorticity (ζ) maxima are attributable to the same event, and that the events last a minimum of 24 hours. Before further analysis, the 6-hourly fields are smoothed with a 12-hour moving window to reduce noise. Those depressions that were not in the IMD eAtlas (`http://www.imdchennai.gov.in/cyclone_eatlas.htm`) were then removed. This gave us 106 IMD tracks between 1979 and 2014 (Fig. 2).

Next, each depression was centralised to 0°N, 0°W and re-oriented using output heading data to create a forward (northward) propagating composite. Rotation during compositing allows us to determine system-relative features and mitigates orographic artifacts, e.g. forced ascent by the Eastern Ghats. We use the term *relative* with compass directions to describe sectors of the depression; relative north being the direction of

*Department of Meteorology, University of Reading, Reading, UK; email: k.hunt@pgr.reading.ac.uk

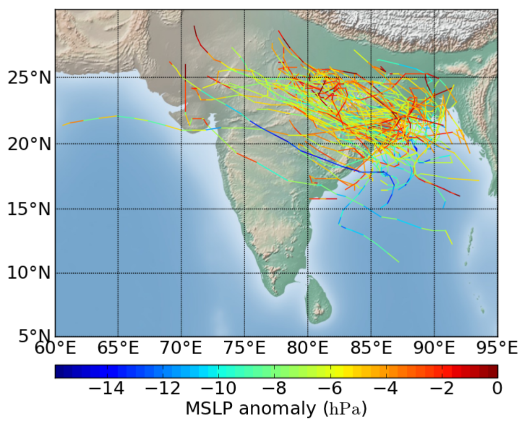

Figure 2: Depression tracks from the 106 depressions used in this study. Colour indicates depression intensity using SLP anomaly to a 21-day running mean.

propagation.

3 COMPOSITE

Using the method previously outlined, we were able to develop a broad three-dimensional composite of the tracked IMDs. These were then sliced horizontally or vertically to illuminate structural features in a broad range of fields. The examples of horizontal structure at the surface given in Fig. 3 show that IMDs can exhibit significant asymmetry, and this is confirmed by examining fields in the vertical (example, Fig. 4). We find that the dominant mode of asymmetry is caused by the presence of the Himalayas, which, for example, causes the winds in the relative east to intensify (as predicted by Hunt and Parker, 2015). Important results from this work include: the discovery of distinct thermal core types in IMDs, with distinct behaviour dependent on the magnitude of the lower-topospheric cold core; that vorticity is strongly confined to the IMD centre; a deep central negative pressure anomaly extending up to ~ 250 hPa; vertical updrafts of over 2 m s^{-1} at the centre; and broad areas of nearly saturated atmosphere.

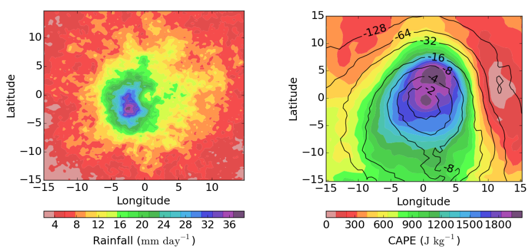

(a) Surface rainfall (b) Surface CAPE and CIN

Figure 3: (a) composite surface rainfall (mm day^{-1}) from TRMM 3B42; (b) CAPE (colours, J kg^{-1}) and CIN (lines, J kg^{-1}) computed from ERA-Interim fields.

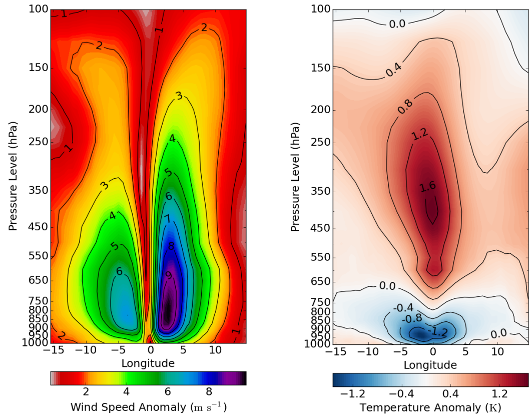

(a) Tangential wind speed (b) Temperature

Figure 4: (a) tangential wind speed (m s^{-1}); (b) temperature (K) as an anomaly to the boreal summmer mean; both shown as slices through the composite centre from relative west to east. Data from ERA-Interim.

4 VARIABILITY

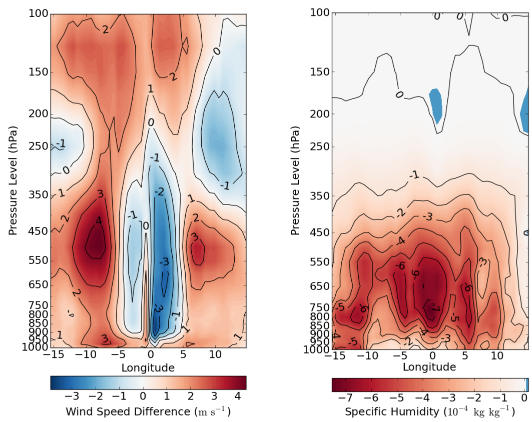

(a) (b)

Figure 5: (a) Tangential wind speed (m s^{-1}) for an ocean-minus-land composite and; (b) specific humidity (10^{-4} kg kg^{-1}) for an El Niño-minus-La Niña composite.

The composite is sufficiently large that it permits exploration of variability from external forcings. Those considered are contrasts with different phases of: ENSO, active-break monsoon cycles, the Indian Ocean Dipole, the diurnal cycle, and land-coast-ocean. We find that the strongest progenitor of variability in almost all fields is the land-sea constrast (Fig. 5(a) shows the difference in tangential wind speed between the two), notably in shape: depressions over the ocean are wider and flatter than over land. The phase of ENSO also has a significant effect (Fig. 5(b) shows the difference in specific humidity between the IMDs in El Niño and La Niña conditions), with IMDs in El Niño being considerably weaker and drier than those during La Niña. Active spells of Indian monsoon act to intensify contemporaneous depressions almost as much as a La Niña event, and we also show that the mean state of the trough on depression days is very similar to that during active periods. The effect of the Indian Ocean Dipole was not found to be significant.

References

Boos, W. R., J. V. Hurley, and V. S. Murthy, 2015: Adiabatic westward drift of Indian monsoon depressions. *Quart. J. Roy. Meteor. Soc.*, **141**, 1035–1048, doi:10.1002/qj.2454.

Ding, Y.-H., 1981: A case study of formation and structure of a depression over the Arabian Sea. *Chin. J. Atmos. Sci.*, **5**, 267–280.

Ding, Y. H., X. Q. Fu, and B. Y. Zhang, 1984: A study of the structure of a monsoon depression over the Bay of Bengal during the summer MONEX. *Adv. Atmos. Sci.*, **1**, 62–75.

Godbole, R., 1977: The composite structure of the monsoon depression. *Tellus*, **29**, 25–40.

Hunt, K. M. R., and D. J. Parker, 2015: The movement of Indian monsoon depressions by interaction with image vortices near the Himalayan wall. *Quart. J. Roy. Meteor. Soc.*, submitted.

Hurley, J. V., and W. R. Boos, 2015: A global climatology of monsoon low pressure system. *Quart. J. Roy. Meteor. Soc.*, **141**, 1049–1064, doi:10.1002/qj.2447.

Prasad, K., S. R. Kalsi, and R. K. Datta, 1990: On some aspects of wind and cloud structure of monsoon depressions. *Mausam*, **41**, 365–370.

Saha, K., F. Sanders, and J. Shukla, 1981: Westward propagating predecessors of monsoon depressions. *Mon. Wea. Rev.*, **109**, 330–343.

Sarker, R. P., and A. Choudhary, 1988: A diagnostic study of monsoon depressions. *Mausam*, **39**, 9–18.

Stano, G., T. N. Krishnamurti, T. S. V. Vijaya Kumar, and A. Chakraborty, 2002: Hydrometeor structure of a composite monsoon depression using the TRMM radar. *Tellus A*, **54**, 370–381, doi:10.1034/j.1600-0870.2002.01330.x.